Journal of Hazardous Materials 179 (2010) 573–580

Contents lists available at ScienceDirect

Journal of Hazardous Materials

journal homepage: www.elsevier.com/locate/jhazmat

Variability of soil potential for biodegradation of petroleum hydrocarbons in a heterogeneous subsurface

Andreas H. Kristensen [a,b,*], Tjalfe G. Poulsen [a], Lars Mortensen [b], Per Moldrup [a]

[a] Aalborg University, Department of Biotechnology, Chemistry, and Environmental Engineering, Sohngaardsholmsvej 57, DK-9000 Aalborg, Denmark
[b] Ramboll Denmark A/S, Sønderbrogade 34, DK-7100 Vejle, Denmark

ARTICLE INFO

Article history:
Received 5 January 2010
Received in revised form 15 February 2010
Accepted 9 March 2010
Available online 16 March 2010

Keywords:
Biological heterogeneity
Petroleum vapors
Spatial variability
Semivariogram analysis
State-space modeling

ABSTRACT

Quantifying the spatial variability of factors affecting natural attenuation of hydrocarbons in the unsaturated zone is important to (i) performing a reliable risk assessment and (ii) evaluating the possibility for bioremediation of petroleum-polluted sites. Most studies to date have focused on the shallow unsaturated zone. Based on a data set comprising analysis of about 100 soil samples taken in a 16 m-deep unsaturated zone polluted with volatile petroleum compounds, we statistically and geostatistically analysed values of essential soil properties. The subsurface of the site was highly layered, resulting in an accumulation of pollution within coarse sandy lenses. Air-filled porosity, readily available phosphorous, and the first-order rate constant (k_1) of benzene obtained from slurry biodegradation experiments were found to depend on geologic sample characterization ($P < 0.05$), while inorganic nitrogen was homogenously distributed across the soil stratigraphy. Semivariogram analysis showed a spatial continuity of 4–8.6 m in the vertical direction, while it was 2–5 times greater in the horizontal direction. Values of k_1 displayed strong spatial autocorrelation. Even so, the soil potential for biodegradation was highly variable, which from autoregressive state-space modeling was partly explained by changes in soil air-filled porosity and gravimetric water content. The results suggest considering biological heterogeneity when evaluating the fate of contaminants in the subsurface.

1. Introduction

Petroleum volatile organic compounds (VOCs) in the unsaturated zone involve risks of: (i) vapor intrusion into residential buildings [1–3] and (ii) gas-phase migration to groundwater aquifers [4–6]. Petroleum VOC concentrations in the soil are generally lowered due to naturally occurring biodegradation, which restricts the volume of soil impacted by a given VOC source [7–9]. This intrinsic soil property suggests the use of bioremediation on sites impacted by petroleum hydrocarbons [10–12]. Since in situ biodegradation rates are closely linked to the availability and distribution of contaminants and external electron acceptors, complex site geology generally reduces the chances of successful bioremediation [11–13]. As a result, detailed information on geologic heterogeneity and spatial variability of essential soil properties in a given petroleum-impacted unsaturated zone is critical to evaluate the fate of contaminants in addition to deciding appropriate remedial measures.

Variable environmental factors prevailing in the unsaturated zone promote tremendous microbial diversity within short spatial distances [14,15]. The distribution of soil microbes is often related to soil depth, as subsoil microbial populations tend to be lower in density and less diverse than surface soil populations [16–18]. On a larger scale, the distribution of microorganisms in the unsaturated zone is often spatially structured over distances of tens to hundreds of meters depending on landscape gradients [19,20]. At the so-called sample-scale of 10–100 mm, a range of biophysical and geochemical conditions in the soil can influence the activity of soil microbes, e.g., moisture content, transport properties, pH, macronutrient concentrations, and availability of natural and synthetic organic compounds [15,21]. At petroleum-contaminated sites in general, two specific limitations of intrinsic biodegradation in the unsaturated zone are reported: (i) availability of oxygen and (ii) availability of macronutrients. The former is related to soil air-filled porosity and distance to the ground level [22–27] whilst the latter is mostly related to nitrogen deficiency in contaminated soil zones where the C: N ratio is high [28–30].

A large number of past studies have analysed the spatial variation of geochemical and soil physical conditions. Some soil properties, including texture and volumetric water content, show considerable spatial structure in the horizontal direction, while variables such as bulk density (ρ_b) and total soil porosity (Φ) do

* Corresponding author at: Aalborg University, Department of Biotechnology, Chemistry, and Environmental Engineering, Sohngaardsholmsvej 57, DK-9000 Aalborg, Denmark. Tel.: +45 40 87 70 56.
E-mail address: anrk@ramboll.dk (A.H. Kristensen).

0304-3894/$ – see front matter © 2010 Elsevier B.V. All rights reserved.
doi:10.1016/j.jhazmat.2010.03.042

not show much spatial correlation in the unsaturated zone [31]. Studies by Iqbal et al. [32] showed that within soil horizons, values for ρ_b and Φ had the lowest variability with a coefficient of variation (CV) around 5%, while for saturated hydraulic conductivity (K_s) it was 160%. Botros et al. [33] investigated the spatial variability of hydraulic properties in a 16 m-deep unsaturated zone. They concluded that the spatial continuity of within-lithofacies variability was about 5–8 m in the horizontal direction and approximately an order of magnitude less in the vertical direction. Nutrient availability in the unsaturated zone is generally reported to decline with depth [16,21]. The spatial variability of NO_3-N in the unsaturated zone was examined by Onsoy et al. [34] who reported highly variable and log-normally-distributed concentration data.

Only a few studies have addressed the variability of soil parameters in subsoils below 2 m [33,34]. More importantly no previous studies have, to the best of our knowledge, examined the spatial continuity and correlation of the soil potential for natural biodegradation in the unsaturated zone, thus leaving a gap in knowledge regarding the effect of heterogeneity on the fate of non-persistent contaminants such as petroleum hydrocarbons. In this study we statistically and geostatistically analyse soil parameters in a petroleum-polluted and 16 m-deep unsaturated zone. The site is previously described in Kristensen et al. [35]. Specifically, the present study (i) characterizes the heterogeneity in site geology and distribution of contaminants; (ii) statistically relates soil potential for biodegradation (measured based on soil slurry experiments amended with benzene), available nitrogen and phosphorous contents, and air-filled porosity to geologic sediment class; (iii) determines the spatial continuity of these parameters based on semivariogram analysis; and (iv) indentifies governing factors of the intrinsic potential for biodegradation based on linear correlations and state-space modeling. The results illustrate conditions that need to be considered when performing investigations of petroleum-impacted sites with a layered unsaturated zone.

2. Materials and methods

2.1. Site description

The study site is located in Nyborg (55°18′42″N, 10°47′31″E), Denmark, at a former gas station. The unsaturated zone is 15.5–16 m thick in the source area and consists of various layers of calcareous glacial deposits. Large amounts of total petroleum hydrocarbons (TPH) of which benzene, toluene, ethylbenzene, and xylene isomers (BTEX) make up 25% were detected in the subsurface in 2001 [35]. The pollution has spread in the unsaturated zone from an underground storage tank and is heterogeneously distributed within an approximately 11 m-thick zone covering an area of 1150 m^2. The ground surface is covered with slabs or asphalt in most of the contaminated area (Fig. 1), and water-phase leaching of contaminants and seasonal water content fluctuations are limited. Also, seasonal groundwater table fluctuations are less than 0.5 m.

2.2. Soil sampling and analysis

In the period between October 2007 and February 2008, drill cores (1000 mm in length and 50 mm in internal diameter) were collected from 7 boreholes using SonicSampDrill® (Fig. 1). The cores were opened and the sample material was visually characterized in terms of soil-type, stratigraphy, occurrence of minor lenses, visual signs of pollution etc. From the soil cores, a total of 100 representative soil samples were collected every 0.5 m (when possible) between 2 and 16 m below ground level (bgl). In addition a total of 19 intact soil cores of 100 cm^3 were collected from major horizontal soil layers before opening the drill cores.

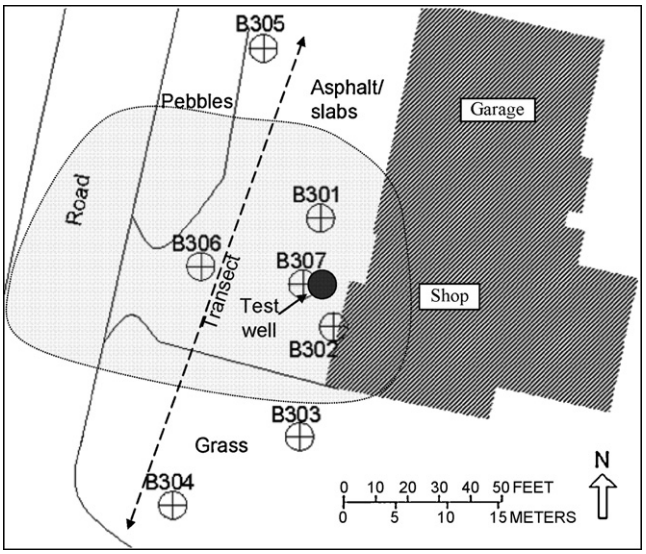

Fig. 1. Outline of the field site and location of boreholes B301-B307. Modified from Ref. [35]. The gray area represents the area with soil contamination.

Soil samples were stored, prepared and analysed as described in Kristensen et al. [35]. Total soil porosity and gas-phase diffusivity (D_p/D_0) were determined on intact soil cores, while inorganic nitrogen (N_{inorg}) and readily available phosphorous (P_{avail}, equal to the so-called *Olsen P*) were determined based on disturbed soil samples. In addition, air-filled porosity for each sample location was calculated from gravimetric water content and total soil porosity, measured on intact cores taken from the same geologic sediment type. The latter is believed to be a valid approach as the within-layer variability of total soil porosity is normally low [32].

The soil potential for biodegradation of petroleum vapors was determined based on aerobic, well-mixed soil slurries with amendment of benzene [35]. A first-order degradation model was fitted to each set of data (dissolved benzene concentration vs. time) and the first-order rate constant (k_1) was established. The value of k_1 reflects the size of the degrading population at the time of the experiments and is related to antecedent environmental conditions influencing soil bacteria in the specific sample location [35].

2.3. Statistical and geostatistical methods

Statistical analyses were performed on data for k_1, ε, N_{inorg}, and P_{avail}. Distribution goodness-of-fit was tested using the Lilliefors test [36]. Mean parameter values determined for main geologic formations in the site were compared using a one-tailed Mann–Whitney test [37] by the data analysis package PAST [38]. The Mann–Whitney test is useful in our case, as it allows a comparison of mean values from data with various statistical distributions.

The spatial continuity, i.e. the semivariance (γ) related to the lag interval (h) between measurements, was evaluated based on classical experimental semivariograms of soil parameters in the vertical and horizontal direction [39]. The semivariograms were fitted to the commonly used spherical model in Eq. (1) [40].

$$\gamma(h) = c_0 + (c - c_0) \cdot \left(\frac{3h}{2a} - 0.5\left(\frac{h}{a}\right)^3 \right), \text{if } 0 \le h \le a\ \gamma(h) = c, h > a \quad (1)$$

where c_0, c, and a are constants corresponding to the nugget, sill, and range of the semivariogram, respectively.

Linear correlation coefficients were determined between any two parameters measured on the same soil sample [40]. Since this approach neglects spatial parameter correlation, an additional

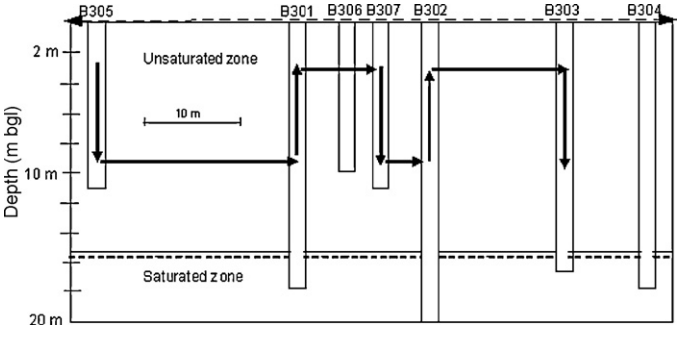

Fig. 2. Construction of composite transects used in state-space modeling.

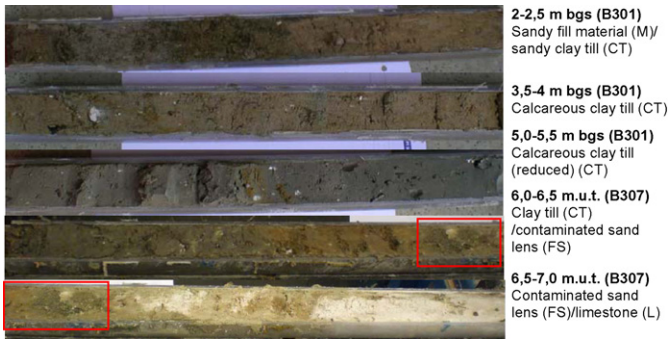

Fig. 3. Examples of soil cores taken at the study site. Red squares denote a contaminated sandy lens.

approach involving autoregressive state-space modeling was used. State-space modeling is based on the simultaneous solution of two sets of equations describing the relation between soil properties at one location and values of the same soil properties in an adjacent location [41]. The method takes into account the uncertainties related to measurement errors. Background theory on state-space modeling is available in Nielsen and Wendroth [40]. Composite transects were constructed for k_1, ε, N_{inorg}, and P_{avail} values measured in the boreholes B305, B301, B307, B302, and B303 (in that order) in depths between 2.5 and 9.5 m. The transects were constructed by connecting the deepest measuring point in the B305 profile with the deepest measuring point in the B301 profile, and then again the top measuring point in B301 with the top measuring point in B307 and so forth (see Fig. 2). In this approach it is assumed that the spatial structure of each parameter does not change significantly, going horizontally from one borehole profile to another nearby borehole. The vertical distance between measuring points was set to 1 m, thus resulting in a total of 40 values of each parameter. Five missing values were generated using linear interpolation of adjacent values. To ensure better convergence of the state-space calculations, measured data (y_i) were scaled with respect to their mean (m) and standard deviation (s) using Eq. (2). This transformation scales the observed data to achieve a mean equal to 0.5 and a standard deviation equal to 0.25 [40].

$$y_{\text{scaled},i} = \frac{y_i - (m - 2s)}{4s} \quad (2)$$

3. Results and discussion

3.1. Geologic and soil physical characterization

3.1.1. Stratigraphy

The top 2 m of the unsaturated zone consisted of sandy fill and was not impacted by pollution. Samples taken from this zone are disregarded in the following analysis. Material obtained between 2 and 16 m bgl were calcareous (10–90% $CaCO_3$) with low contents of natural organic matter (<0.15%). The grain size ranged from clay and limestone to coarse sand, and covered a wide spectrum of textures in between. Texturally different geologic units were typically layered in the horizontal direction with thicknesses varying from <10 cm for some sandy lenses to >2 m for major layers of limestone and glacial till. Examples of drill cores are shown in Fig. 3. Based on field descriptions of texture, color, and degree of sorting, sample materials were divided into main sediment classes. Of 100 soil samples collected, 80 could be classified as clay till (CT), fine sand (FS), or limestone (L). The remaining 20 variably textured samples were classified as "miscellaneous" (M), covering materials of coarse sand, clay-rich sand, and well-sorted silt. Typical depths and physical characteristics of main sediment classes are shown in Table 1.

3.1.2. Main sediment classes

The texture of clay till (CT) materials was heterogeneous with approximately 10% comprising of gravel, stones, and pieces of flint and chalk. The remaining soil particles included 13% clay, 49% sand, 10% silt, and 29% $CaCO_3$ (Table 1). Even though precipitated iron oxides indicated presence of macropores or fractures in several samples, no large cracks or openings were noted during soil characterization. Samples of fine sand (FS) were generally well-sorted with 75% fine sand (20–200 μm) and about 13% $CaCO_3$. Samples classified as limestone (L) were generally white and soft with high water content (close to saturation). The $CaCO_3$ content in these materials was typically >70%. However, a limestone layer located near the groundwater table had a grayish color and a $CaCO_3$ content ranging from 50% to 60%.

3.1.3. Distribution of contamination

Distribution of total petroleum hydrocarbons (TPH) in the unsaturated zone was closely related to the soil layering as demonstrated in Fig. 3. High concentrations (>1000 mg TPH/kg) were associated with sandy lenses on top of water-bearing sediments of silt and limestone, an observation also reported from previous studies [42–44]. Concentrations ranging up to 1000 mg TPH/kg were randomly distributed in deposits of FS and L, while samples consisting of CT generally contained <10 mg TPH/kg. However, laboratory measurements detected trace concentrations of petroleum vapors in the majority of samples taken in CT deposits. Furthermore, field measurements showed vapor concentrations ranging up to 5700 μg TPH/L soil air in geologic formations of CT [35]. Even with the majority of pollution accumulated in coarse lenses, these results illustrate that petroleum vapors spread in fine-textured CT deposits. This is in agreement with measurements of gas-phase diffusivity (D_p/D_0) in undisturbed samples of CT (Table 1), where D_p is the gas diffusion coefficient in soil and D_0 is the gas diffusion coefficient in free air. These showed an D_p/D_0 around 0.02 for in situ moisture conditions, thereby demonstrating possible gas-phase transport of oxygen and petroleum vapors [35]. On the other hand, low D_p/D_0 in water-bearing limestone suggests these deposits represent impermeable vapor barriers. In summary, the complex geology of the unsaturated zone at the study site played an essential role for the distribution of contamination 'hot spots' and for the gas-phase migration pathways of petroleum vapors.

3.2. Statistical and geostatistical analysis

3.2.1. Variations within and among sediment classes

Table 2 shows the results following statistical analyses of first-order benzene rate constants (k_1), soil air-filled porosity (ε), available nitrogen (N_{inorg}), and available phosphorous (P_{avail}) measured for 100 sample locations. Macronutrient concentrations were low as expected for low-organic subsurface conditions [30]. Even

Table 1
Soil texture and physical characteristics of main sediment classes. Modified from Ref. [35].

Main sediment class	*n*	CT	FS	L	M
Typical depth of formation (m bgs)	–	2–10	10–13	5–9 and 13 -15	2–16
Clay (<2 μm) (kg kg^{-1})	8	0.132	0.043	n/a	n/a
Silt (2–20 μm) (kg kg^{-1})	8	0.096	0.022	n/a	n/a
Fine sand (20–200 μm) (kg kg^{-1})	8	0.252	0.753	n/a	n/a
Coarse sand (200–2000 μm)	8	0.236	0.051	n/a	n/a
$CaCO_3$ (kg kg^{-1})	8	0.291	0.130	>0.500	n/a
Soil organic matter (kg kg^{-1})	8	0.0019	0.0012	n/a	n/a
Gravimetric water content (kg kg^{-1})	100	0.140 (0.029)	0.115 (0.039)	0.187 (0.041)	0.157 (0.0471)
Dry bulk density[a] (g cm^{-3})	19	1.75	1.59	1.71	1.65
Total soil porosity[a] (cm^3 cm^{-3})	19	0.34	0.40	0.35	0.36
Gas diffusivity (D_p/D_0) (−100 cm H_2O)[a]	19	0.021 (0.025)	0.031 (0.071)	0.007 (0.017)	0.009 (0.035)

[a] Dry bulk density, total soil porosity and gas diffusivity are determined on 19 intact 100 cm^3 soil cores.

so, benzene degradation in laboratory slurries occurred with k_1 values ranging up to 5 d^{-1} and with an arithmetic mean of 1.5 d^{-1}. These rates are relatively high compared to previously reported values [35]. At the same time, k_1 was the parameter exhibiting the highest coefficient of variation (CV) at 118% with a number of samples showing no evidence of biodegradation within the timeframe of the experiments (i.e. 75 h). This reflects major sample-scale variability of the biological potential for natural attenuation of pollutants.

Fig. 4 shows the density functions for all data together as well as for individual sediment classes. Values for P_{avail} and N_{inorg} were generally log-normally distributed with a positive skew (Table 2), in line with findings of Onsoy et al. [34]. Values for k_1 and ε were more randomly distributed. The Lilliefors test ($P < 0.05$) showed that these parameters were normally distributed within deposits of CT and L.

A one-tailed Mann–Whitney test ($P < 0.05$) suggested mean values of k_1 to be related to geologic sediment class in the order CT > FS > L. This is in line with previous findings showing higher microbial abundance, enzymatic activity, and batch biodegradation rates in clayey soils than in sandy soils [45,46]. The low microbial activity in samples classified as L is likely due to water contents close to saturation ($\varepsilon < 6\%$), which effectively restricts aerobic biodegradation and growth of soil bacteria. The results illustrate that zones of high intrinsic potential for biodegradation and zones with no potential can both be present within a singe soil profile depending on geologic and soil physical conditions. In addition, the evident texture-effect on the soil potential for biodegradation suggests the need to use texture-dependent biodegradation rates when setting up risk assessment models for a layered subsurface. Likewise, biodegradation rates during remedial strategies relying on natural or stimulated biodegradation will most likely vary between different geologic soil layers of the site.

3.2.2. Spatial continuity

The spatial continuity of profile data of k_1, ε, N_{inorg}, and P_{avail} (a maximum of 100 measuring points) was determined using a classical semivariogram analysis similar to the approach applied by Botros et al. [33], which is suitable for irregularly-spaced data. Directional semivariograms based on all data were constructed with the maximum lag distance (h) set to 6 m in the vertical direction and 43 m in the horizontal direction. In the horizontal direction, data pairs of samples collected in depths ±0.5 m from each other were accepted. Semivariance ($\gamma(h)$) values based on fewer than four pairs were discarded.

As some lag distances, typically the lower values, occur more frequently than others, the reliability of the semivariance estimates will vary from each point [39]. Such a situation gives rise to inconsistencies and/or experimental fluctuations in the semivariograms which are, by definition, nondecreasing functions [40]. This was also the case for most parameters in this study as seen in Fig. 5. The experimental semivariograms are fitted to the spherical model (Eq. (1)) with the model parameters given in Table 3. The model generally provided a reasonable fit, except for N_{inorg} data in the horizontal direction, where a pure nugget effect was observed. This corresponds to the total absence of autocorrelation on the scale used in this study (3.75 m < h < 38 m). Other semivariograms showed a low nugget compared to sill, thus indicating a strong spatial correlation and an adequate sampling frequency [32]. Generally, the sill of the vertical semivariograms is similar or close to that of the horizontal

Table 2
Statistical analysis of first-order rate constants (k_1), air-filled porosity (ε), available phosphorous (P_{avail}), and inorganic nitrogen (N_{inorg}).

Variable	Main sediment class	*n*	Mean	Min.	Max.	Median	Skewness	SD	CV (%)	Prob. Dist.[a]
k_1 (d^{-1})	All data	97	1.50	0.00	5.09	0.67	1.53	1.76	118	–
	CT	40	2.25	0.00	5.09	2.10	0.23	1.52	68	Norm.
	FS	17	0.90	0.02	4.43	0.33	2.07	1.26	140	Log-norm.
	L	18	0.083	0.00	0.54	0.049	2.81	0.131	157	Norm.
ε (cm^3 cm^{-3})	All data	77	0.11	0.00	0.31	0.11	0.23	0.08	69	Norm.
	CT	39	0.094	0.01	0.17	0.10	-0.49	0.04	46	Norm.
	FS	15	0.19	0.09	0.27	0.20	-0.14	0.06	29	Log-norm.
	L	16	0.058	0.00	0.16	0.0052	0.49	0.070	120	–
P_{avail} (mg kg^{-1})	All data	98	4.34	0.53	43.37	3.38	6.23	4.69	108	Log-norm.
	CT	39	3.61	0.87	12.46	3.30	2.35	2.02	56	Log-norm.
	FS	17	2.14	0.53	4.17	1.97	0.38	0.93	44	Log-norm.
	L	20	6.39	2.46	13.51	6.24	0.94	2.72	43	Log-norm.
N_{inorg} (mg kg^{-1})	All data	100	1.11	0.56	2.75	1.06	1.23	0.43	38	Log-norm.
	CT	46	1.09	0.56	2.29	0.99	1.02	0.41	37	Log-norm.
	FS	15	1.13	0.58	2.31	1.09	1.44	0.42	37	Norm.
	L	20	1.16	0.61	1.53	1.33	−0.66	0.32	27	Log-norm.

[a] Best fit of the normal or log-normal distribution confirmed by the Lilliefors test ($P < 0.05$)

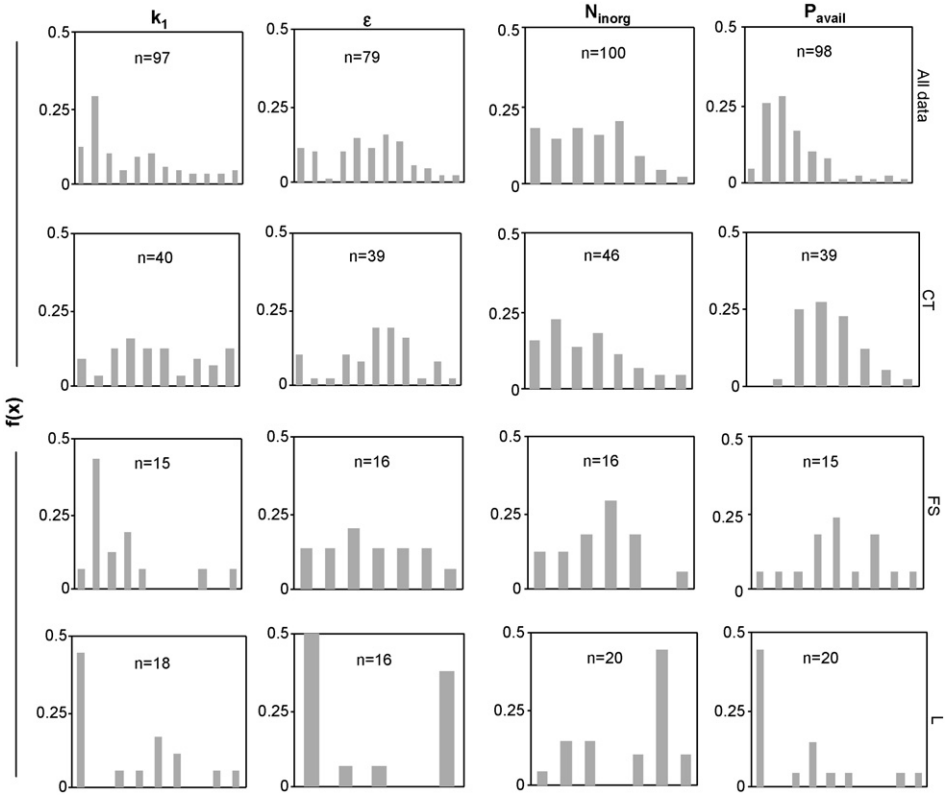

Fig. 4. Density functions for first-order rate constants (k_1), air-filled porosity (ε), available phosphorous (P_{avail}), and inorganic nitrogen (N_{inorg}). Plots are shown for all data together as well as for individual sediment classes. The *x*-axes correspond to the range (i.e., min. and max. values) listed in Table 2.

direction. The geostatistical range, however, is 2–4 times greater in the horizontal direction than that in the vertical direction, suggesting anisotropy related to horizontal soil layering. This demonstrates the need for extensive sampling in the vertical direction during site investigation in a layered subsurface.

Strongest spatial dependence is estimated for k_1 that has a vertical range of 8.6 m and a horizontal one of 35.8 m. As these values are close to or exceed the maximum lag intervals used, biodegradation potentials measured in samples from any two locations in the study site are likely to be geostatistically related, despite considerable variability. The spatial continuity for the biodegradation potential is stronger than previously observed for hydraulic properties in deep subsurface alluvial soils [33]. This illustrates that long-term contamination with volatile petroleum compounds most likely has a profound effect on the abundance and activity of soil bacteria on the whole site, while hydraulic and soil physical properties of any given geologic deposit will generally be static and unlikely to change over time. The latter is particularly the case when the surface pavement prevents noteworthy infiltration through the unsaturated zone as is the case at the study site.

3.2.3. Parameter correlations

For the complete set of data representing all soil classes combined, no evident linear correlations between any two parameters were observed ($R^2 < 0.1$) (data not shown). This demonstrates the complexity of the site geology. Table 4 shows observed linear correlation coefficients (R) within samples of CT alone, representing about 40% of the complete data set. Values for $k_1 < 0.6$ d^{-1} (8 samples) were disregarded, as absence of degradation in these samples was likely to be related with factors not considered in this study, in particular, toxic effects due to high petroleum concentrations [35]. The most evident correlation in CT deposits was observed between ε and k_1 (Fig. 6). The relatively strong fit ($R = 0.84$) suggests local diffusion limitation of oxygen and petroleum vapors in

Table 3
Best-fit parameters determined with the spherical semivariogram model.

Variable	Nugget (c_0)	Sill (c)	Range (a), m	Cross validation R	Nugget/sill
k_1					
Vertically	0.94	2.56	8.6	0.92	0.37
Horizontally	0.04	2.50	35.8	0.92	0.06
ε					
Vertically	0.0021	0.0095	4.4	0.84	0.22
Horizontally	0	0.0055	17.8	0.91	0.00
P_{avail}					
Vertically	0.55	9.1	4.7	0.83	0.06
Horizontally	0	6.1	9.8	0.59	0.06
N_{inorg}					
Vertically	0.028	0.12	4.0	0.74	0.24
Horizontally	0.35	–	–	–	–

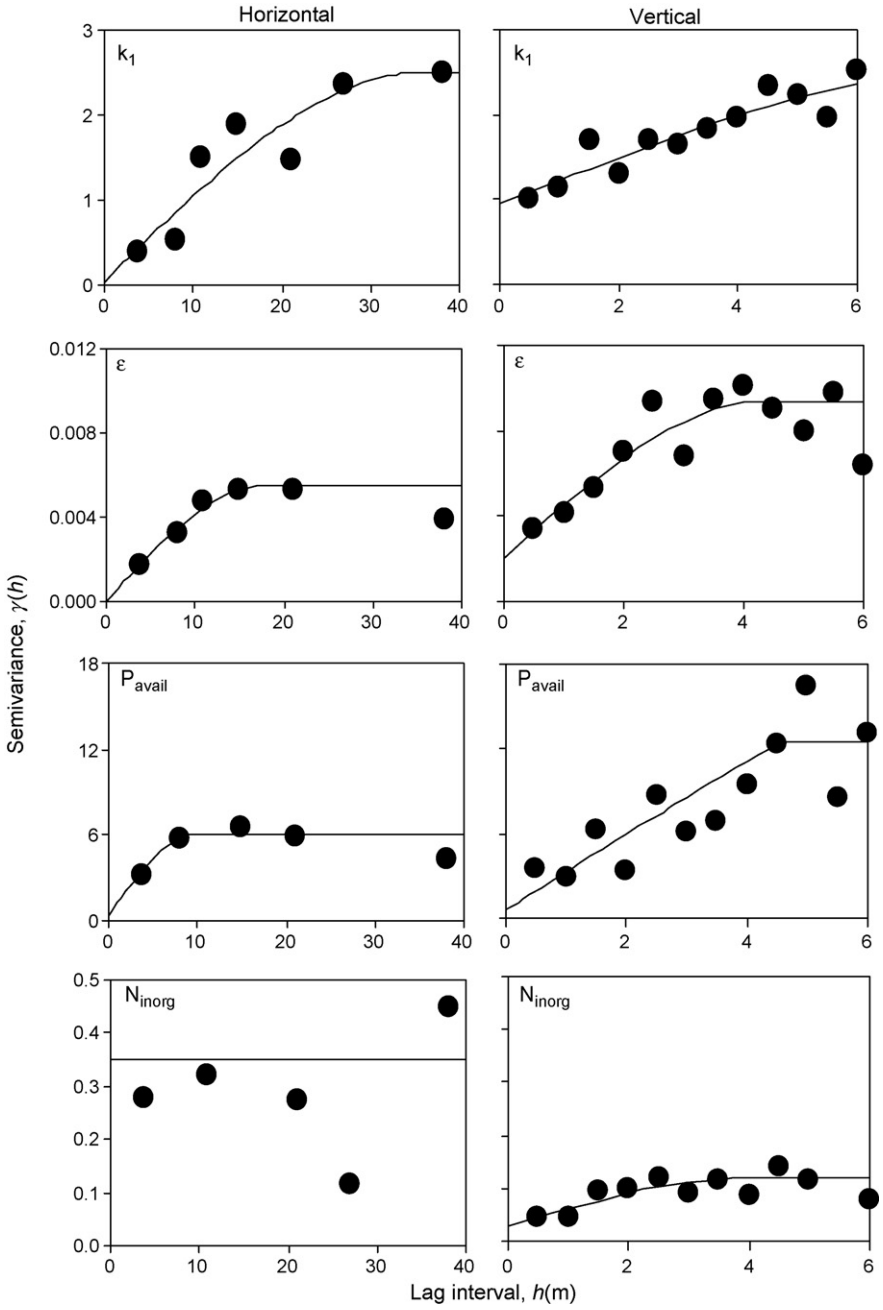

Fig. 5. Experimental semivariograms and best-fits of the spherical model (Eq. (1)).

these sediments, which has restricted antecedent aerobic growth of soil bacteria. As a result, deposits with high water content appear to create zones with limited aerobic biodegradation activity [47]. A negative correlation between N_{inorg} and ε indicate that inorganic nitrogen is mainly found in the soil water. This in turn means a negative correlation between k_1 and N_{inorg}.

Table 4
Linear correlation coefficients (R) in samples consisting of clay till (CT).

	k_1	ε	N_{inorg}	P_{avail}
k_1	–			
ε	0.84	–		
N_{inorg}	−0.55	−0.53	–	
P_{avail}	0.18	0.22	0.04	–
z	−0.04	−0.11	0.22	0.62

Since the semivariogram analysis suggested strong spatial correlation of k_1, accuracy of the prediction at a given sample location is likely to be improved if measurements at adjacent sample locations are considered. A state-space modeling approach was used to predict k_1 from neighboring values of k_1 and one additional parameter (ε, N_{inorg}, P_{avail}, soil depth (z) or gravimetric water content (ω)) along a transect consisting of 40 sample locations. Of these, 25 were in deposits of CT, 7 in layers of L, and 2 in sandy lenses. Table 5 shows model expressions and goodness-of-fit in terms of the root mean square error (RMSE). Whilst the majority of the estimated k_1 values at a given location can be explained by the neighboring k_1 values, contributions derived from the spatial correlation structure of other neighboring parameters were relatively small. In line with the results of the semivariogram analysis (Table 3), state-space data suggest that the value of k_1 depends on a number of variables and has a strong spatial autocorrelation. Soil depth and N_{inorg} both

Table 5
Contributions to the first-order rate constant (k_1) derived from the spatial correlation structure of other neighboring parameters.

Parameter affecting k_1	Model expression	RMSE	Contribution (%)[a]
Air-filled porosity, ε	$k_{1,i+1} = 1.09k_{1,i} - 0.12\varepsilon_i$	0.201	9.74
Inorganic nitrogen, N_{inorg}	$k_{1,i+1} = 0.92k_{1,i} + 0.056N_{inorg,i}$	0.195	5.68
Available phosphorous, P_{avail}	$k_{1,i+1} = 0.90k_{1,i} + 0.083P_{avail,i}$	0.185	8.52
Soil depth, z	$k_{1,i+1} = 1.013k_{1,i} - 0.051z_i$	0.196	4.76
Gravimetric water content, ω	$k_{1,i+1} = 0.81k_{1,i} + 0.17\omega_i$	0.156	17.4

[a] Contribution (α) = $|B|/(|A| + |B|)$, where $k_{1,i+1} = Ak_{1,i} + B\alpha_i$.

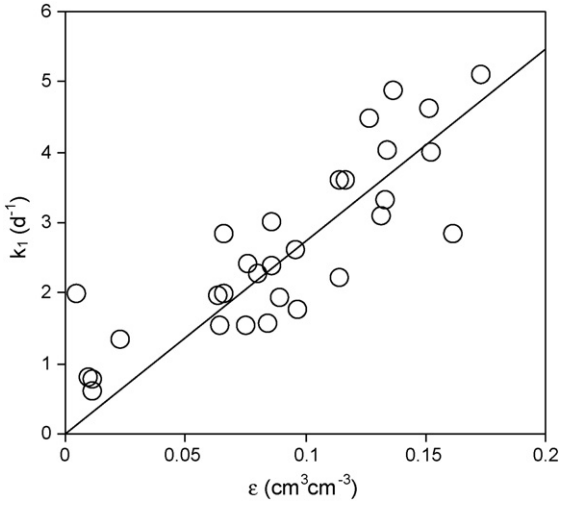

Fig. 6. Values for k_1 plotted against air-filled porosity (ε) in the same sample location. Values for $k_1 < 0.6$ d^{-1} were disregarded in this analysis.

explained less than 6% of the k_1 values, while P_{avail} explained 8.5% and ε explained 9.7%. Since phosphorous concentrations are related to soil class (Table 2), the effect of P_{avail} is likely to be a soil-type effect rather than an indication of phosphorous being the main limiting factor [35]. Based on the strong linear relationship between k_1 and ε determined in samples of CT, the 9.7% contribution found in the state-space results from neighboring ε values was less than expected. Also, Fig. 7a shows a poor fit of k_1 data. It is noticed that the model underestimates high values and overestimates low values, a finding commonly observed when performing state-space modeling [41]. Most evident contribution to the biodegradation potential was obtained from the gravimetric water content (ω) at 17.4%. Fig. 7b shows the model results based on neighboring values of k_1 and ω, which to some extent were able to predict the highly fluctuating k_1 data. Since the contribution by ω is higher than the one derived from the physical phase distribution (i.e., values of ε), the gravimetric water content is likely to represent factors apart from water saturation, namely, soil texture and organic matter content. This is in line with the relationship observed between main sediment class and k_1 (Table 3) and suggests the biodegradation potential within a petroleum-contaminated geologic formation to be an intrinsic property related to soil texture in addition to the availability of pollutants and oxygen.

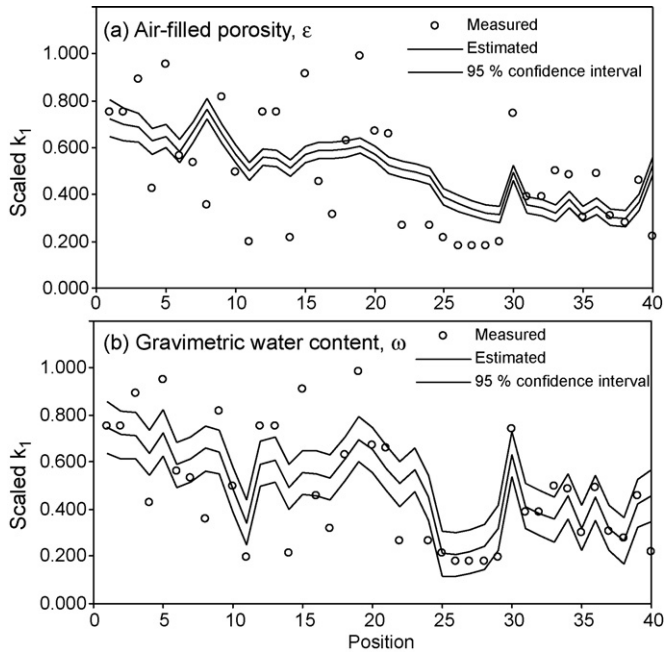

Fig. 7. Results of state-space model runs based on the first-order rate constant (k_1) and (a) air-filled porosity (ε) and (b) gravimetric water content. The y-axes represent values scaled according to Eq. (2).

4. Conclusions

Understanding the heterogeneity and variability of soil properties in a contaminated subsurface is critical to assessing short and long-term risks posed by contaminants. In this study we statistically and geostatistically analysed a comprehensive set of data including essential soil parameters likely to affect intrinsic biodegradation in a 16 m-deep petroleum-polluted unsaturated zone. The site is interesting because (i) hydrocarbon-degrading bacteria will be dominant due to low contents of natural organic matter, and (ii) the distribution of contaminant hot spots and vapors at this site is strongly affected by a complex stratigraphy with most of the contaminants accumulated in coarse lenses within less permeable deposits.

Air-filled porosity, readily available phosphorous, and the soil potential for aerobic biodegradation in a given geologic formation were related to geological classification ($P < 0.05$), while inorganic nitrogen was more homogenously distributed, independent of soil texture. Since an unsaturated zone is likely to contain zones with high as well as low potential for biodegradation, modeling intrinsic biodegradation in the field, i.e., when performing risk assessments, requires the use of texture-dependent biodegradation kinetics. Directional semivariogram analysis of measured soil parameters showed that spatial continuities were 2–5 times greater in the horizontal than in the vertical direction, demonstrating that a layered subsurface requires frequent soil sampling in the vertical direction. First-order degradation rate constants (k_1) displayed strong spatial autocorrelation, which suggests microbial populations at the whole site to be affected by the contamination. However the soil potential for biodegradation in each sample location was related to air-filled porosity and gravimetric water content, in line with the relationship observed between sediment class and k_1. Collectively, results from this study suggest measurements of total soil porosity, gravimetric water content, and microcosm studies of biodegradation potentials in all major geologic formations to add useful information to the conceptual site model. This will reveal if biological heterogeneity in the subsurface needs to be consid-

ered in a risk assessment or during future remedial strategies at the site.

Acknowledgements

We wish to thank Helle Blendstrup and Hanna Gerlach for analytical assistance. Thanks also to Ben Newton for reviewing early drafts of this manuscript. This work was funded by Ramboll Denmark A/S and The Danish Agency for Science, Technology and Innovation under the Industrial PhD Programme.

References

[1] M.L. Fischer, A.J. Bentley, K.A. Dunkin, A.T. Hodgson, W.W. Nazaroff, R.G. Sextro, J.M. Daisey, Factors affecting indoor air concentrations of volatile organic compounds at a site of subsurface gasoline contamination, Environ. Sci. Technol. 30 (1996) 2948–2957.
[2] I. Hers, J. Atwater, L. Li, R. Zapf-Gilje, Evaluation of vadose zone biodegradation of btx vapours, J. Contam. Hydrol. 46 (2000) 233–264.
[3] B.M. Patterson, G.B. Davis, Quantification of vapor intrusion pathways into a slab-on-ground building under varying environmental conditions, Environ. Sci. Technol. 43 (2009) 650–656.
[4] A.L. Baehr, P.E. Stackelberg, R.J. Baker, Evaluation of the atmosphere as a source of volatile organic compounds in shallow groundwater, Water Resour. Res. 35 (1999) 127–136.
[5] G. Pasteris, D. Werner, K. Kaufmann, P. Hohener, Vapor phase transport and biodegradation of volatile fuel compounds in the unsaturated zone: a large scale lysimeter experiment, Environ. Sci. Technol. 36 (2002) 30–39.
[6] M. Christophersen, M.M. Broholm, H. Mosbaek, H.K. Karapanagioti, V.N. Burganos, P. Kjeldsen, Transport of hydrocarbons from an emplaced fuel source experiment in the vadose zone at airbase v ae rlose, Denmark, J. Contam. Hydrol. 81 (2005) 1–33.
[7] P. Hohener, N. Dakhel, M. Christophersen, M. Broholm, P. Kjeldsen, Biodegradation of hydrocarbons vapors: comparison of laboratory studies and field investigations in the vadose zone at the emplaced fuel source experiment, airbase vaerlose, Denmark, J. Contam. Hydrol. 88 (2006) 337–358.
[8] L.D.V. Abreu, P.C. Johnson, Effect of vapor source – building separation and building construction on soil vapor intrusion as studied with a three-dimensional numerical model, Environ. Sci. Technol. 39 (2005) 4550–4561.
[9] G.E. Devaull, Indoor vapor intrusion with oxygen-limited biodegradation for a subsurface gasoline source, Environ. Sci. Technol. 41 (2007) 3241–3248.
[10] R.E. Hinchee, D.C. Downey, R.R. Dupont, P.K. Aggarwal, R.N. Miller, Enhancing biodegradation of petroleum hydrocarbons through soil venting, J. Hazard. Mater. 27 (1991) 315–325.
[11] D.C. Downey, R.E. Hinchee, R.N. Miller, Cost-effective Remediation And Closure Of Petroleum-Contaminated Sites, Battelle Press, Columbus, Ohio, 1999.
[12] R. Boopathy, Factors limiting bioremediation technologies, Bioresour. Technol. 74 (2000) 63–67.
[13] P. Hohener, D. Hunkeler, A. Hess, T. Bregnard, J. Zeyer, Methodology for the evaluation of engineered in situ bioremediation: lessons from a case study, J. Microbiol. Methods 32 (1998) 179–192.
[14] P.S. Giller, The diversity of soil communities, the 'poor man's tropical rainforest', Biodivers. Conserv. 5 (1996) 135–168.
[15] D. Or, B.F. Smets, J.M. Wraith, A. Dechesne, S.P. Friedman, Physical constraints affecting bacterial habitats and activity in unsaturated porous media – a review, Adv, Water Resour. 30 (2007) 1505–1527.
[16] A. Konopka, R. Turco, Biodegradation of organic compounds in vadose zone and aquifer sediments, Appl. Environ. Microbiol. 57 (1991) 2260–2268.
[17] T.L. Bone, D.L. Balkwill, Morphological and cultural comparison of microorganisms in surface soil and subsurface sediments at a pristine study site in oklahoma, Microbiol. Ecol. 16 (1988) 49–64.
[18] J.Z. Zhou, B.C. Xia, H. Huang, A.V. Palumbo, J.M. Tiedje, Microbial diversity and heterogeneity in sandy subsurface soils, Appl. Environ. Microbiol. 70 (2004) 1723–1734.
[19] F.J. Brockman, C.J. Murray, Symposium on Subsurface Microbiology, Davos, Switzerland, September 15–21, 1996.
[20] C.H. Ettema, D.A. Wardle, Spatial soil ecology, Trends Ecol. Evol. 17 (2002) 177–183.
[21] P.A. Holden, N. Fierer, Microbial processes in the vadose zone, Vadose Zone J. 4 (2005) 1–21.
[22] S. Roggemans, C.L. Bruce, P.C. Johnson, R.L. Johnson, Vadose zone natural attenuation of hydrocarbon vapors: An empirical assessment of soil gas vertical profile data, Vol. Bulletin No. 15, American Petroleum Institute, Washington, D.C., 2001.
[23] G.B. Davis, J.L. Rayner, M.G. Trefry, S.J. Fisher, B.M. Patterson, Measurement and modeling of temporal variations in hydrocarbon vapor behavior in a layered soil profile, Vadose Zone J. 4 (2005) 225–239.
[24] G.B. Davis, B.M. Patterson, M.G. Trefry, Evidence for instantaneous oxygen-limited biodegradation of petroleum hydrocarbon vapors in the subsurface, Ground Water Monit. Rem. 29 (2009) 126–137.
[25] H. Luo, P. Dahlen, P.C. Johnson, T. Peargin, T. Creamer, Spatial variability of soil-gas concentrations near and beneath a building overlying shallow petroleum hydrocarbon-impacted soils, Ground Water Monit. Rem. 29 (2009) 81–91.
[26] M.H. Huesemann, M.J. Truex, The role of oxygen diffusion in passive bioremediation of petroleum-contaminated soils, J. Hazard. Mater. 51 (1996) 93–113.
[27] P.D. Lundegard, P.C. Johnson, P. Dahlen, Oxygen transport from the atmosphere to soil gas beneath a slab-on-grade foundation overlying petroleum-impacted soil, Environ. Sci. Technol. 42 (2008) 5534–5540.
[28] J.T. Dibble, R. Bartha, Leaching aspects of oil sludge biodegradation in soil, Soil Sci. 127 (1979) 365–370.
[29] R. Xu, J.P. Obbard, Effect of nutrient amendments on indigenous hydrocarbon biodegradation in oil-contaminated beach sediments, J. Environ. Qual. 32 (2003) 1234–1243.
[30] K. Kaufmann, M. Christophersen, A. Buttler, H. Harms, P. Hohener, Microbial community response to petroleum hydrocarbon contamination in the unsaturated zone at the experimental field site vaerlose, Denmark, Fems Microbiol. Ecol. 48 (2004) 387–399.
[31] M. Duffera, J.G. White, R. Weisz, Spatial variability of southeastern us coastal plain soil physical properties: implications for site-specific management, Geoderma 137 (2007) 327–339.
[32] J. Iqbal, J.A. Thomasson, J.N. Jenkins, P.R. Owens, F.D. Whisler, Spatial variability analysis of soil physical properties of alluvial soils, Soil Sci. Soc. Am. J. 69 (2005) 1338–1350.
[33] F.E. Botros, T. Harter, Y.S. Onsoy, A. Tuli, J.W. Hopmans, Spatial variability of hydraulic properties and sediment characteristics in a deep alluvial unsaturated zone, Vadose Zone J. 8 (2009) 276–289.
[34] Y.S. Onsoy, T. Harter, T.R. Ginn, W.R. Horwath, Spatial variability and transport of nitrate in a deep alluvial vadose zone, Vadose Zone J. 4 (2005) 41–54.
[35] A.H. Kristensen, K. Henriksen, L. Mortensen, K.M. Scow, P. Moldrup, Soil physical constraints on intrinsic biodegradation of petroleum vapors in a layered subsurface, Vadose Zone J. 9 (2010) 1–11.
[36] H.W. Lilliefors, On Kolmogorov-Smirnov test for normality with mean and variance unknown, J. Am. Stat. Assoc. 62 (1967), 399-&.
[37] H.B. Mann, D.R. Whitney, On a test of whether one of 2 random variables is stochastically larger than the other, Ann. Math. Statistics 18 (1947) 50–60.
[38] Ø. Hammer, D.A.T. Harper, P.D. Ryan, Past: Paleontological statistics software package for education and data analysis, Palaeontologia Electronica 4 (2001).
[39] Z. Sen, Cumulative semivariogram models of regionalized variables, Mathematical Geol. 21 (1989) 891–903.
[40] D.R. Nielsen, O. Wendroth, Spatial And Temporal Statistics: Sampling Field Soils And Their Vegetation, Catena Verlag GMBH, Reiskirchen, Germany, 2003.
[41] T.G. Poulsen, P. Moldrup, O. Wendroth, D.R. Nielsen, Estimating saturated hydraulic conductivity and air permeability from soil physical properties using state-space analysis, Soil Sci. 168 (2003) 311–320.
[42] R.A. Dawe, M.R. Wheat, M.S. Bidner, Experimental investigation of capillary-pressure effects on immiscible displacement in lensed and layered porous-media, Transport Porous Media 7 (1992) 83–101.
[43] D.H. Phillips, A.O. Thomas, K. Forde, K. Dickson, S. Plant, G. Norris, B. Bone, R.M. Kalin, Fate and transport of volatile organic compounds in glacial till and groundwater at an industrial site in northern Ireland, Environ. Geol. 52 (2007) 1117–1131.
[44] J.L. Smith, D.D. Reible, Y.S. Koo, E.P.S. Cheah, Vacuum extraction of a nonaqueous phase residual in a heterogeneous vadose zone, J. Hazard. Mater. 49 (1996) 247–265.
[45] J.P. Taylor, B. Wilson, M.S. Mills, R.G. Burns, Comparison of microbial numbers and enzymatic activities in surface soils and subsoils using various techniques, Soil Biol. Biochem. 34 (2002) 387–401.
[46] M.E. Watwood, C.S. White, C.N. Dahm, Methodological modifications for accurate and efficient determination of contaminant biodegradation in unsaturated calcareous soil, Appl. Environ. Microbiol. 57 (1991) 717–720.
[47] J. Skopp, M.D. Jawson, J.W. Doran, Steady-state aerobic microbial activity as a function of soil-water content, Soil Sci. Soc. Am. J. 54 (1990) 1619–1625.